Journal of AL-Qadisiyah for computer science and mathematics Vol.10 No.2 Year 2018
ISSN (Print): 2074 – 0204 ISSN (Online): 2521 – 3504

Analysis of Heat Transfer on Peristaltic Transport of Powell- Eyring Fluid in an Inclined Tapered Symmetric Channel with Hall and Ohm's Heating Influences

Hayat A. Ali **Ahmed M. Abdulhadi**

University of Baghdad, College of Science, Department of Mathematics

hayattadel17@yahoo.com **ahm6161@yahoo.com**

Recived : 18\12\2017 **Revised : 28\12\2017** **Accepted : 10\1\2018**

Available online : 17 /2/2018

DOI: 10.29304/jqcm.2018.10.2.364

Abstract

In this paper, we present an analysis of heat transfer on peristaltic flow for Powell- Eyring fluid in an inclined symmetric tapered channel is discussed. Hall effect, velocity, thermal slip conditions, and Ohm's heating are taken into consideration. The governing equations for the balance of mass, momentum and energy are modeled, and then simplified by holding the consideration of long wavelength and low Renolds number approximation. Graphical results are given to analyze the behavior of the parameters emerging in the problem. Effect of Hall parameter and Hartman number on velocity axial have opposite characteristics.

Key words: Heat Transfer, Hall Effect, Ohm's Heating, Powell- Eyring Fluid, Tapered Channel.

Subject Classification: 80Axx, 76Dxx, 76Txx.

1. Introduction

Peristaltic transport in recent times has collected a considerable attention due to its application in physiological, engineering, and biological systems. The peristalsis in general refers to sequential longitudinal and circular contractions of sinusoidal induced peristaltic waves that propagate along the channel that contains the fluid. Particularly this mechanism is the basis of many muscle tubes such as gastrointestinal tract, fallopian tube, bile duct, ureter and esophagus tube etc. Moreover it has a key role in many industrial applications like transport of sanitary fluid, blood pumps in heart lung machines, corrosive fluids transport [1,2] . As well as non- Newtonian fluid is considered to be more suitable than the Newtonian fluids in many industrial and physiological processes [3-5]. Varieties of non-Newtonian fluid models (exhibiting different rheological effects) are available and amongst those is the Powell- Eyring fluid [6]. Even this model is mathematically more complex, but deserves more consideration because of its distinct advantages over the non- Newtonian fluid models. Recently, numerous effective researches have been presented for the peristaltic flow of Powell- Eyring fluid under the assumptions of large wavelength and low Renolds number and with different flow conditions (see refs.[7-9]).The heat transfer refers to the exchange of the thermal energy among the different components of the system. However its rate depends on the temperature of various compartment and physical properties of the flow medium. The study of the influence of heat transfer on non -Newtonian fluids has become important in last years. This importance is due to numerous of industrial processes. Examples are food processing biochemical operations and transport in polymers, biomedical engineering, micro fabrication technologies [5]. Besides this the phenomenon of peristalsis with heat transfer has a wide spread applications in mechanical engineering, physiological processes as oxygenation and hemodialysis, diffusion of chemical impurities. In view of the above considerable applications many researches have been reported the heat transfer analysis in peristaltic motion for different non-Newtonian fluid and flow geometries. Ramesh and Devakar in [10] investigated the effect of heat transfer on the peristaltic transport of MHD second grade model through porous medium in an inclined symmetric channel. Hayat et al in [11] studied the heat transfer analysis in peristaltic flow of Prandtl- Eyring fluid through a curved channel. Veerakrishna et al in.[12] discussed the heat transfer with peristaltic flow of Williamson fluid under the effect of inclined magnetic field in a symmetric planar channel. Ghash in [13] adopted a heat transfer of Newtonian fluid through a rotating channel under the impact of Hall effect and transfer magnetic field. Hina in [8] explored the combined influences of slip and MHD on peristaltic motion of Eyring-Powell fluid with taken into consideration heat/ mass transfer. Abbasi et al.in [14] addressed the heat transfer in hydromagnetic peristaltic flow of variable viscosity fluid through porous medium. Also, Hina et al.in [9] investigates the heat transfer in the peristaltic transport of Powell- Eyring fluid inside a curved channel and its application in biomedicine.

The Hall current effect is considerable when Hall parameter is high. This can be achieved in a strong magnetic field. The Hall current has a remarkable effect on Lorentz force term. This effect is employed in numerous aspects like astrophysical, meteorological, MHD power generations, plasma flow problem and centrifugal machines. Motivated by such fact the influence of the Hall current on the flow can be seen via studies [5,13,15,16].Another considerable aspect in peristalsis is the non-uniform (tapered) flow configuration. This configuration is noticed in most practical applications like physiological body organs, small blood vessels, intestines, lymphatic vessels and ducts afferents. Blood flow suspension for Walter's B fluid model through tapered stenosed arteries discussed by Akbar in [17]. Influence of variable viscosity on MHD peristaltic flow of Pseudoplastic fluid model through a tapered symmetric channel studied by [18]. Further recent literature can be seen via refs. [3,19,20]. This work addresses heat transfer analysis of peristaltic flow of conducting Powell- Eyring model in an inclined tapered symmetric channel under the effect of Hall current. The mathematical model formulation is subjected to a transverse magnetic field presence. Besides this the energy equation is modeled by taking Joule (Ohm's) heating impact into account. The two-dimensional equations of motion and energy are simplified by adopting lubrication approach. The governing equation is carried out by utilizing long wavelength approximation and low Renolds number assumptions. The series solution of the stream function, axial velocity, heat transfer and temperature distribution have been obtained by employing the perturbation technique. The major behavior of Hartman number, Hall parameter, Froude number, Renold number, inclination of angle, phase difference, non-uniform parameter and Powell- Eyring fluid parameters on velocity profile, temperature, heat transfer and the peristaltic flow are analyzed in detail graphically.

2. Problem Mathematical description

Assume the peristaltic transport of an incompressible Powell- Eyring fluid in two-dimensional tapered symmetric channel of thickness $2d$. The channel is taken inclined at angle α to the horizontal axis. The fluid is electrically conducting in the presence of a strong applied magnetic field $B = (0,0,\beta_0)$. The magnetic Renolds number is taken a very low approximation hence the induced magnetic field is neglected. Symmetry in the flow achieved by the peristaltic waves with different amplitude and phases moving with a constant speed c and wavelength λ along the walls of the channel. Hall and Ohm's heating effects are taken into account.

The structure of walls geometry are described as:

$$Y_1 = H_1(X,\bar{t}\,) = d + \bar{m}_1 X + a\sin(\frac{2\pi}{\lambda}\,(X - c\bar{t}\,) + \phi) \quad (1)$$

$$Y_2 = H_2(X,\bar{t}\,) = d + \bar{m}_1 X + b\sin(\frac{2\pi}{\lambda}\,(X - c\bar{t}\,)) \quad (2)$$

In which Y_1, Y_2 are the lower and upper wall respectively, a, b are the amplitudes of waves along the lower and upper walls, $\bar{m}_1 (\ll 1)$ the non- uniform parameter.

The Cartesian coordinates (X, Y) in such a way that wave propagates in X- direction and Y – axis is taken normal to it. $\phi \in [0, \pi]$ the phase difference. Moreover $\phi = 0$ corresponds to symmetric channel with waves out of phase, and $\phi = \pi$ describes the waves in phase. Further a, b, d and ϕ satisfy the inequality so that the walls still parallel.

$$a^2 + b^2 + 2abd\cos\emptyset \leq (2d)^2 \quad (3)$$

The fluid is obeying the Powell- Eyring model and the Cauchy stress tensor $\bar{\tau}$ of it is given as follows

$$\bar{\tau} = -\bar{P}I + \bar{S} \quad (4)$$

$$\bar{S} = \left[\mu + \frac{1}{\beta\dot{\gamma}} sinh^{-1}\left(\frac{\dot{\gamma}}{c_1}\right)\right] A_1 \quad (5)$$

$$\dot{\gamma} = \sqrt{\frac{1}{2}\, tra({A_1}^2)} \quad (6)$$

$$A_1 = \nabla\vec{V} + (\nabla\vec{V})^T \quad (7)$$

Where $\bar{S}$ express the extra stress tensor, I the identity tensor $\nabla = (\partial X, \partial Y, 0)$ the gradient vector, β, c_1 the material parameters of Powell-Eyring fluid, and μ the dynamic viscosity. The term $sinh^{-1}$ can be approximated as

$$sinh^{-1}\left(\frac{\dot{\gamma}}{c_1}\right) = \frac{\dot{\gamma}}{c_1} - \frac{\dot{\gamma}^3}{6{c_1}^3}, \left|\frac{\dot{\gamma}^5}{{c_1}^5}\right| \ll 1 \quad (8)$$

Applying the generalized Ohm's law, including the Hall current we get

$$\vec{J} = \sigma[\vec{V} \times \vec{B} - \frac{1}{en}(\vec{J} \times \vec{B})] \quad (9)$$

$$\vec{J} \times \vec{B} = \left(\frac{-\sigma{\beta_0}^2(U - mV)}{1+m^2} i - \frac{\sigma{\beta_0}^2(V + mU)}{1+m^2} j\right) \quad (10)$$

In which $\vec{J}$ characterize the current density vector, $\vec{V} = (U, V, 0)$ the velocity field, σ the electrical conductivity, n the number density of electron, e the electric charge, β_0 the magnetic field strength and $\left(m = \frac{\sigma\beta_0}{en}\right)$ the Hall parameter.

The balance of mass, momentum and temperature are given respectively below

$$\frac{\partial U}{\partial X} + \frac{\partial V}{\partial Y} = 0 \quad (11)$$

$$\rho\left(\frac{\partial U}{\partial \bar{t}} + U\frac{\partial U}{\partial X} + V\frac{\partial U}{\partial Y}\right) = \frac{\partial \bar{P}}{\partial X} + \frac{\partial \bar{S}_{XX}}{\partial X} + \frac{\partial \bar{S}_{XY}}{\partial Y} - \frac{\sigma{\beta_0}^2(U - mV)}{1+m^2} + \rho g\, sin\alpha \quad (12)$$

$$\rho\left(\frac{\partial V}{\partial \bar{t}} + U\frac{\partial V}{\partial X} + V\frac{\partial V}{\partial Y}\right) = \frac{\partial \bar{P}}{\partial Y} + \frac{\partial \bar{S}_{YX}}{\partial X} + \frac{\partial \bar{S}_{YY}}{\partial Y} - \frac{\sigma{\beta_0}^2(V + mU)}{1+m^2} + \rho g\, cos\alpha \quad (13)$$

and

$$\rho c_P\left(\frac{\partial T}{\partial \bar{t}} + U\frac{\partial T}{\partial X} + V\frac{\partial T}{\partial Y}\right) = k\left(\frac{\partial^2 T}{\partial X^2} + \frac{\partial^2 T}{\partial Y^2}\right) + (\bar{S}_{YY} - \bar{S}_{XX})\frac{\partial V}{\partial Y} + \bar{S}_{XY}\left(\frac{\partial U}{\partial Y} + \frac{\partial V}{\partial X}\right) + \frac{\sigma{\beta_0}^2(U^2+V^2)}{1+m^2} \quad (14)$$

Where

$\bar{t}, \rho, \bar{P}, \vec{J}, g, c_P, T, k, \sigma, \vec{J} \times \vec{B}, \frac{\vec{J}.\vec{J}}{\sigma}, (U, V, 0)$ are time, fluid density, pressure, current density, the gravity, the specific heat, temperature, thermal conductivity, the electrical conductivity, the component of Lorentz force, Joule heating component, and the velocity components corresponding to the laboratory frames $(X, Y, \bar{t})$,also $\bar{S}_{ij}$ represents the components of stress tensor and $(i = X\,,\ j = Y)$.

The components of extra stress tensor of Powell- Eyring defined by Eq.(5) are listed below

$$\bar{S}_{XX} = 2\left(\mu + \frac{1}{\beta c_1}\right)U_X - \frac{1}{3\beta{c_1}^3}[2{U_X}^2 + (U_Y + V_X)^2 + 2{V_Y}^2]U_X \quad (15)$$

Journal of AL-Qadisiyah for computer science and mathematics Vol.10 No.2 Year 2018
ISSN (Print): 2074 – 0204 ISSN (Online): 2521 – 3504

$$\bar{S}_{XY} = \left(\mu + \frac{1}{\beta c_1}\right)(V_X + U_Y) - \frac{1}{6\beta {c_1}^3}\left[2{U_X}^2 + (U_Y + V_X)^2 + 2{V_Y}^2\right](V_X + U_Y) \qquad (16)$$

$$\bar{S}_{YY} = 2\left(\mu + \frac{1}{\beta c_1}\right)V_Y - \frac{1}{3\beta {c_1}^3}\left[2{U_X}^2 + (U_Y + V_X)^2 + 2{V_Y}^2\right]V_Y \qquad (17)$$

The corresponding boundary conditions are listed below

The slip conditions for velocity and temperature at the walls are

$$U \pm \gamma \bar{S}_{XY} = 0 \quad \text{at } Y = H_1 \text{ and } Y = H_2 \qquad (18)$$

$$T \pm \beta_1 \frac{\partial T}{\partial Y} = T_0 \quad \text{at } Y = H_1 \text{ and } Y = H_2 \qquad (19)$$

Flexible walls are given as

$$\left[-\tau \frac{\partial^3}{\partial X^3} + m_2 \frac{\partial^3}{\partial X \partial \bar{t}^2} + d' \frac{\partial^2}{\partial \bar{t} \partial X}\right] Y = \frac{\partial \bar{S}_{XX}}{\partial X} + \frac{\partial \bar{S}_{XY}}{\partial Y} - \rho\left(\frac{\partial U}{\partial \bar{t}} + U\frac{\partial U}{\partial X} + V\frac{\partial U}{\partial Y}\right) - \frac{\sigma {\beta_0}^2 (U - mV)}{1+m^2} + \rho g \sin\alpha \quad , Y = H_1 \text{ and } Y = H_2 \qquad (20)$$

In which $T_0, \tau, m_2, d', \gamma, \beta_1$ are the temperature at the upper and lower walls, the elastic tension, the mass per unit area, the coefficient of viscous damping, the velocity slip parameter, and the thermal slip parameter respectively.

The dimensionless quantities are defined as

$$x = \frac{X}{\lambda}, y = \frac{Y}{d}, u = \frac{U}{c}, v = \frac{V}{c}, h_1 = \frac{H_1}{d}$$
$$h_2 = \frac{H_2}{d}, p = \frac{d^2 \bar{p}}{\lambda \mu c}, \delta = \frac{d}{\lambda}, \gamma^* = \frac{\gamma}{d}, \beta_1^* = \frac{\beta_1}{d}$$
$$S = \frac{d\bar{S}(X)}{\mu c}, R1 = \frac{\rho c d}{\mu}, W = \frac{1}{\mu \beta c_1}, A = \frac{W}{6}\left(\frac{c}{c_1 d}\right)^2$$
$$\theta = \frac{T - T_0}{T_0}, E_1 = \frac{-\tau d^3}{\lambda^3 \mu c}, E_2 = \frac{m_2 c d^3}{\lambda^3 \mu c}, E_3 = \frac{d' d^3}{\lambda^2 \mu}$$
$$Pr = \frac{\mu c_P}{k}, H = \beta_0 d \sqrt{\frac{\sigma}{\mu}}, E_c = \frac{c^2}{c_P T_0}, Br = E_c Pr,$$
$$a^* = \frac{a}{d}, b^* = \frac{b}{d}, \quad m_1 = \frac{\overline{m}_1 \lambda}{d}, Fr = \frac{c}{\sqrt{gd}} \qquad (21)$$

Where

$\delta, E_1, E_2, E_3, R1, Pr, H, Ec, Br, Fr, m_1, P, h_1, h_2, x, y, u, v, A, W, \gamma^*, \beta_1^*$ are the wave number, the wall elastance parameter, the mass per unit area parameter, the wall damping parameter, the Renolds number, the Prandtl number, Hartman number, Eckret number, Brinkman number, Froude number, the dimensionless non- uniform parameter, the dimensionless pressure, the dimensionless lower wall surface, upper wall surface, components of the dimensionless coordinates, axial velocity, transverse component of velocity, the Eyring-Powell fluid dimensionless parameters ,the dimensionless velocity and thermal slip parameters respectively. Note that asterisks will be omitted for simplicity.

The stream function $\psi(x, y, t)$ and its connection with velocity components is scripted below

$$u = \frac{\partial \psi}{\partial y} \quad and \quad v = -\delta \frac{\partial \psi}{\partial x} \qquad (22)$$

Substituting Eq.(21) into Eqs.(11) – (20) and make use of Eq.(22), note that the mass balance represented by Eq. (11) is identically satisfied, yields

Journal of AL-Qadisiyah for computer science and mathematics Vol.10 No.2 Year 2018
ISSN (Print): 2074 – 0204 ISSN (Online): 2521 – 3504

$$\delta R1(\psi_{ty} + \psi_y\psi_{xy} - \delta\psi_x\psi_{xy}) = -P_x + \delta\frac{\partial S_{xx}}{\partial x} + \frac{\partial S_{xy}}{\partial y} - \frac{H^2}{(1+m^2)}(\psi_y + \delta m\psi_x) + \frac{R1}{(Fr)^2}\, sin\alpha \quad (23)$$

$$\delta^2 R1(-\delta^2\psi_{tx} - \delta^2\psi_y\psi_{xx} + \delta^3\psi_x\psi_{xy}) = P_y + \delta\frac{\partial S_{yy}}{\partial y} + \delta^2\frac{\partial S_{yx}}{\partial x} - \frac{H^2\delta}{(1+m^2)}(-\delta\psi_x + m\psi_y) + \frac{R1}{(Fr)^2}\, cos\alpha \quad (24)$$

$$PrR1\left(\delta\frac{\partial\theta}{\partial t} + \delta\psi_y\frac{\partial\theta}{\partial x} - \delta\psi_x\frac{\partial\theta}{\partial y}\right) = \delta^2\frac{\partial^2\theta}{\partial x^2} + \frac{\partial^2\theta}{\partial y^2} + BrS_{xy}(\psi_{yy} - \delta^2\psi_{xx}) + \frac{H^2 Br}{(1+m^2)}((\psi_y)^2 + \delta^2(\psi_x)^2) + \delta Br(S_{xx} - S_{yy})\psi_{xy} \quad (25)$$

The dimensionless of stress components can be given by

$$S_{xx} = \delta(1+W)\psi_{xy} - \delta A\left[\delta^2\psi_{yx}^2 + \frac{1}{4}(\psi_{yy} - \delta^2\psi_{xx})^2 + \delta^2\psi_{xy}^2\right]\psi_{xy} \quad (26)$$

$$S_{xy} = (1+W)(-\delta^2\psi_{xx} + \psi_{yy}) - \left[4A\delta^2(-\delta^2\psi_{xx} + \psi_{yy})\psi_{xy}^2 + A(-\delta^2\psi_{xx} + \psi_{yy})^3 + 2A\delta^2\psi_{yx}^2(-\delta^2\psi_{xx} + \psi_{yy})\right] \quad (27)$$

$$S_{yy} = -\delta(1+W)\psi_{xy} + 4A\delta\left[\delta^2\psi_{xy}^2 + (\psi_{yy} - \delta^2\psi_{xx})^2 + \delta^2\psi_{xy}^2\right]\psi_{xy} \quad (28)$$

The corresponding dimensionless boundary conditions are listed below

$$\left.\begin{matrix}\psi_y - \gamma\left((1+W)\psi_{yy} - A\psi_{yy}^3\right) = 0 \\ \theta - \beta_1\theta_y = 0\end{matrix}\right\}$$

at $y = h_1$ (29)

$$\left.\begin{matrix}\psi_y + \gamma\left((1+W)\psi_{yy} - A\psi_{yy}^3\right) = 0 \\ \theta + \beta_1\theta_y = 0\end{matrix}\right\}$$

at $y = h_2$ (30)

and

$$\left[E_1\frac{\partial^3}{\partial x^3} + E_2\frac{\partial^3}{\partial x\partial t^2} + E_3\frac{\partial^2}{\partial t\partial x}\right]y = \frac{\partial S_{xy}}{\partial y} - \frac{H^2\psi_y}{1+m^2} + \frac{R1}{(Fr)^2}sin\alpha \quad \text{at } y = h_1 \;\;, y = h_2 \quad (31)$$

The dimensionless forms of lower and upper walls are

$$h_1(x) = -(1 + m_1 x + a\sin(2\pi(x-t) + \phi)) \quad (32)$$

$$h_2(x) = (1 + m_1 x + b\sin(2\pi(x-t))) \quad (33)$$

Employing authentic long wavelength and low Renolds number approximations we obtain

$$-P_x + \frac{\partial S_{xy}}{\partial y} - \frac{H^2\psi_y}{1+m^2} = 0 \quad (34)$$

$$P_y = 0 \quad (35)$$

$$\frac{\partial^2\theta}{\partial y^2} + BrS_{xy}\psi_{yy} + \frac{H^2 Br}{(1+m^2)}(\psi_y)^2 = 0 \quad (36)$$

Eq.(35) indicates that the pressure is independent of the non- dimensional coordinate y . Differentiate Eq. (34) w. r. t y and make use of Eq. (35), the equations which govern the problem are

$$\frac{\partial^2 S_{xy}}{\partial y^2} - \frac{H^2}{(1+m^2)}\psi_{yy} = 0 \quad (37)$$

$$\frac{\partial^2\theta}{\partial y^2} + BrS_{xy}\psi_{yy} + \frac{H^2 Br}{(1+m^2)}(\psi_y)^2 = 0 \quad (38)$$

$$\left.\begin{matrix}\psi_y - \gamma\left((1+W)\psi_{yy} - A\psi_{yy}^3\right) = 0 \\ \theta - \beta_1\theta_y = 0\end{matrix}\right\}$$

at $y = h_1$
(39)

$$\left.\begin{matrix}\psi_y + \gamma\left((1+W)\psi_{yy} - A\psi_{yy}^3\right) = 0 \\ \theta + \beta_1\theta_y = 0\end{matrix}\right\}$$

at $y = h_2$
(40)

and

$$\left[E_1\frac{\partial^3}{\partial x^3} + E_2\frac{\partial^3}{\partial x\partial t^2} + E_3\frac{\partial^2}{\partial t\partial x}\right]y = \frac{\partial S_{xy}}{\partial y} - \frac{H^2\psi_y}{1+m^2} + \frac{R1}{(Fr)^2}sin\alpha \quad \text{at } y = h_1 \;\;, y = h_2 \quad (41)$$

Journal of AL-Qadisiyah for computer science and mathematics Vol.10 No.2 Year 2018
ISSN (Print): 2074 – 0204 ISSN (Online): 2521 – 3504

Heat transfer coefficient at the lower wall is defined as

$$Z = \frac{\partial h_1}{\partial x}\,\theta_y(h_1) \tag{42}$$

3. Solution Technique

Now using the perturbation technique for small Eyring- Powell parameter A by expanding the flow quantities in a power series of A in such manner

$$\psi = \psi_0 + A\,\psi_1 + \cdots \tag{43}$$

$$\theta = \theta_0 + A\,\theta_1 + \cdots \tag{44}$$

Substituting Eqs.(44), (45) into Eqs.(37) - (42) and then comparing the coefficients of same power of A up to the first order we obtain the following two system.

3.1. Zeroth order system

The general form of zeroth- order system is

$$(1+W)\psi_{0yyyy} - \frac{H^2}{(1+m^2)}\psi_{0yy} = 0 \tag{45}$$

$$\theta_{0yy} + Br(1+W)\left(\psi_{0yy}\right)^2 + \frac{H^2 Br}{(1+m^2)}\left(\psi_{0y}\right)^2 = 0 \tag{46}$$

with the respective boundary conditions

$$\left.\begin{array}{c}\psi_{0y} - \gamma(1+W)\psi_{0yy} = 0\\ \theta_0 - \beta_1\theta_{0y} = 0\end{array}\right\}\ \text{at } y = h_1 \tag{47}$$

$$\left.\begin{array}{c}\psi_{0y} + \gamma(1+W)\psi_{0yy} = 0\\ \theta_0 + \beta_1\theta_{0y} = 0\end{array}\right\}\ \text{at } y = h_2 \tag{48}$$

$$\left[E_1\frac{\partial^3}{\partial x^3} + E_2\frac{\partial^3}{\partial x\partial t^2} + E_3\frac{\partial^2}{\partial t\partial x}\right]y = (1+W)\psi_{0yyyy} - \frac{H^2\psi_{0y}}{1+m^2} + \frac{R1}{(Fr)^2}sin\alpha$$

$$\text{at } y = h_1 \text{ and } y = h_2 \tag{49}$$

By solving the above systems for ψ_0 and θ_0, the final form solution for the zeroth order are

$$\psi_0 = \frac{1}{{N_1}^2}\left(e^{N_1 y}c_1 + e^{-N_1 y}c_2\right) + c_3 + c_4 y \tag{50}$$

$$\theta_0 = -Br(1+W)\left(\frac{1}{2{N_1}^2}\left({c_2}^2 e^{-2N_1 y} + {c_1}^2 e^{2N_1 y}\right) + \frac{1}{N_1}\left(-2c_2c_4e^{-N_1 y} + 2c_1c_4e^{N_1 y}\right) + \frac{{c_4}^2{N_1}^2y^2}{2}\right) + b_1 + yb_2 \tag{51}$$

3.2. The First Order System

The first order system has the form

$$(1+W)\psi_{1yyyy} - \frac{H^2}{(1+m^2)}\psi_{1yy} - \frac{\partial^2}{\partial y^2}\left(\psi_{0yy}\right)^3 = 0 \tag{52}$$

$$\theta_{1yy} + Br\left(2(1+W)\psi_{0yy}\psi_{1yy} - \left(\psi_{0yy}\right)^4\right) + \frac{2H^2Br}{(1+m^2)}\psi_{0y}\psi_{1y} = 0 \tag{53}$$

Along with the appropriate boundary condition

$$\left.\begin{array}{c}\psi_{1y} - \gamma\left((1+W)\psi_{1yy} - \left(\psi_{0yy}\right)^3\right) = 0\\ \theta_1 - \beta_1\theta_{1y} = 0\end{array}\right\}\ \text{at } y = h_1 \tag{54}$$

$$\left.\begin{array}{c}\psi_{1y} + \gamma\left((1+W)\psi_{1yy} - \left(\psi_{0yy}\right)^3\right) = 0\\ \theta_1 + \beta_1\theta_{1y} = 0\end{array}\right\}\ \text{at } y = h_2 \tag{55}$$

$$(1+W)\psi_{1yyy} - \frac{\partial}{\partial y}\left(\psi_{0yy}\right)^3 - \frac{H^2}{(1+m^2)}\psi_{1y} = 0 \quad \text{at } y = h_1 \text{ and } y = h_2 \tag{56}$$

Solving the above system for first order the final calculated expressions for ψ_1 and θ_1 are

$$\psi_1 = \frac{1}{8(1+W){N_1}^2}\,e^{-3N_1 y}(L_1 + L_2) + c_7 + c_8 y \tag{57}$$

$$\theta_1 = \left(\frac{-Br}{24{N_1}^2}\right)e^{-4N_1 y}\,(L_3 + L_4 + L_5) + b_3 + b_4 y \tag{58}$$

Where

$$N_1 = \frac{H}{\sqrt{(1+W)(1+m^2)}}, \quad W \geq 0$$

$$L_1 = \left({c_2}^3 + 6c_2{c_1}^2e^{4N_1 y}(-5 + 2N_1 y) - 6{c_2}^2c_1e^{2N_1 y}(5 + 2N_1 y)\right)$$

$$L_2 = e^{2N_1 y}\left({c_1}^3e^{4N_1 y} + 8(1+W)\left(e^{2N_1 y}\,c_5 + c_6\right)\right)$$

$$L_3 = 3{c_2}^4 + 36c_1{c_2}^2c_4N_1e^{3N_1 y}\,(7 + 2N_1 y) - {c_2}^3e^{N_1 y}\left(2c_4N_1 + 3c_1e^{N_1 y}(29 + 12N_1 y)\right)$$

$$L_4 = e^{3N_1 y}\left(3{c_1}^4e^{5N_1 y} + 2{c_1}^3c_4e^{4N_1 y}N_1 + 24c_1e^{2N_1 y}(1+W)\left(c_5e^{N_1 y} + 2c_8N_1\right) + 24c_4N_1(1+W)\left(-2c_6 + 2c_5e^{2N_1 y} + c_8e^{N_1 y}y^2{N_1}^3\right)\right)$$

Journal of AL-Qadisiyah for computer science and mathematics Vol.10 No.2 Year 2018
ISSN (Print): 2074 – 0204 ISSN (Online): 2521 – 3504

$$L_5 = 3c_2 e^{2N_1 y}\left(8c_6(1+W) + e^{N_1 y}\left(-16c_8(1+W)N_1 + 12{c_1}^2 c_4 e^{2N_1 y} N_1(-7 + 2N_1 y) + {c_1}^3 e^{3N_1 y}(-29 + 12N_1 y)\right)\right)$$

4. Results and Discussions

This section transmits the graphical description of various parameters on the outcomes flow quantities. The variation of streamlines, axial velocity, temperature, and heat transfer coefficient are demonstrate and analyzed graphically.

4.1. Velocity Distribution

The development of axial velocity in response to involved parameters has been recorded for fixed values $(x = 0.2,\ t = 0.1)$ through the Figs. (1 to 7). All the profiles are parabolic about the channel's width due to zero displacement at the boundaries. Fig.(1) inspects the impact of wall properties parameters E_1 , E_2 and E_3 on velocity profile. It is noticed that for ascending values of E_1 , E_2 and E_3 the axial velocity tends to increase. The influence of fluid parameters A on the velocity profile is portrayed in Fig. (2,). It is seen that the velocity is increasing function for parameter (A) The effect of Hartman number (H) is sketched in Fig.(3). Reduction behavior for $u(y)$ is recognized as (H) increases. This outcome is due to the Lorentz force which opposes the fluid motion and hence reduces the velocity profile. Fig. (4) is plotted to study the effect of Hall parameter (m) on the velocity profile. One can observed that the velocity increases as the Hall parameter increases this due to the fact that the Hall effect balances the resistive influence of applied magnetic field. Fig. (5) has been sketched to notice the behavior of velocity profile upon various values of channel phase angle (ϕ). It is observed that the velocity increases in the entire tapered channel for ascending values of (ϕ). Fig. (6) is drawn to analyze the impact of amplitude of lower wall (a) on the velocity profile. This figure indicates that an increase in (a) the axial velocity increases near the lower wall for $-1.2 \le y \le -0.95$. However the velocity decreases in the rest of the channel $-0.8 \le y \le 1.2$ with higher values of (a). The velocity profile upon the non- uniform parameter (m_1) is plotted in Fig. (7). We observed that the velocity value increases as the magnitude of non- uniform parameter (m_1) increases

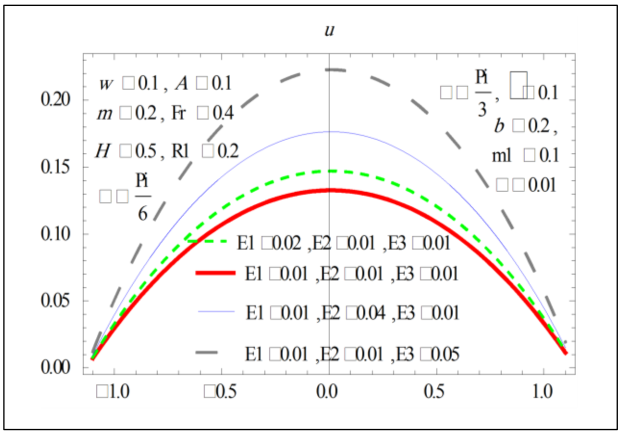

Fig.(1) Velocity Profile with Wall properties

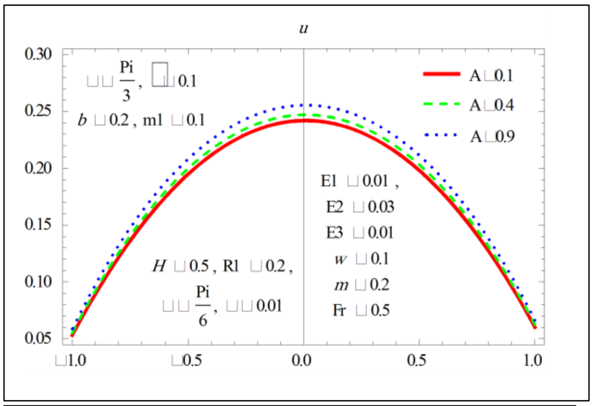

Fig.(2) Velocity Profile Via variation of A

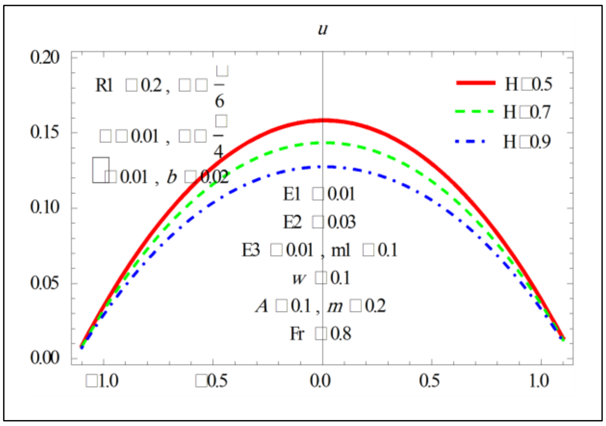

Fig.(3) Velocity Profile Via variation of H

Journal of AL-Qadisiyah for computer science and mathematics Vol.10 No.2 Year 2018
ISSN (Print): 2074 – 0204 ISSN (Online): 2521 – 3504

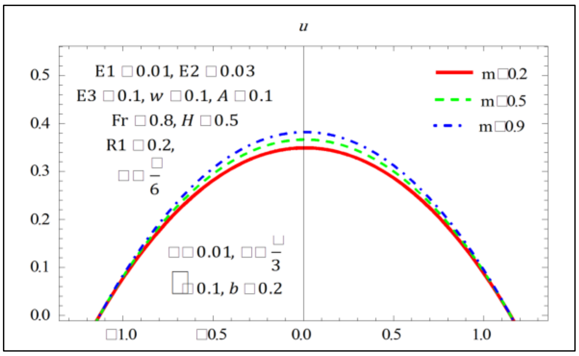

Fig.(4) Velocity Profile Via variation of m

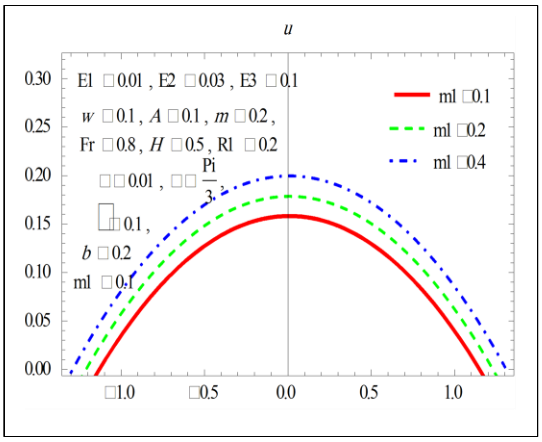

Fig.(7) Velocity Profile Via m_1

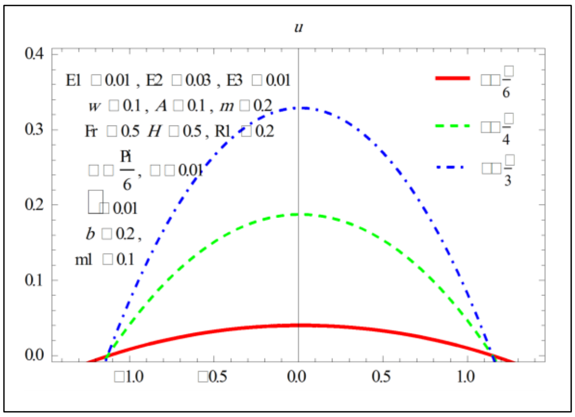

Fig.(5) Velocity Profile Via ϕ

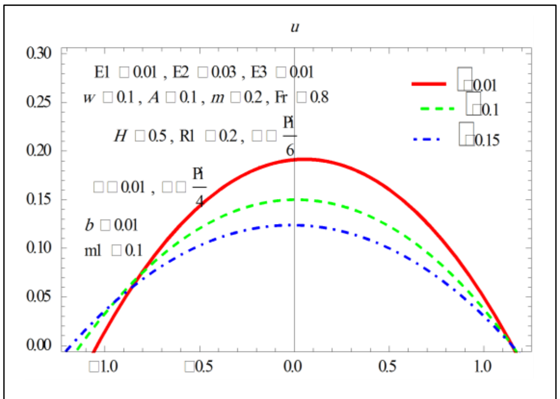

Fig.(6) Velocity Profile Via a

4.2. Temperature Distribution

The quantitative effects of different emerging parameters on temperature distribution $\theta(y)$ are observed physically at fixed values $(x = 0.2, t = 0.1)$via Figs. (8 - 13) . It is analyzed through the figures that $\theta(y)$ attains a maximum value near the central part of the channel.. The variation in temperature with an increase in material fluid parameter A is discussed in Fig.(8). Since the temperature is defined as average kinetic energy of molecules hence ascending values of A causes a risen in θ values. Figs.(9 and 10) is devoted to explain the influence of variation of both channel inclination (α) and phase angle (ϕ).It is observed that θ is rising with an increase in (α) magnitude but opposite attitude is recorded for (ϕ). Higher values of Brinkman number (Br) leads the temperature distribution to grow up see Fig.(11). However the temperature profile decreases for larger values of Froude number (Fr) through Fig.(12). The impact of Hall parameter (m) is captured in Fig.(13).

It is revealed that $\theta(y)$ increases with the increase of (m) near the lower and upper walls for specific at $-1.2 \leq y \leq -0.4 \cup 0.6 \leq y \leq 1.2$ whereas decline in temperature is noticed with growing in Hall parameter at the central part of the channel.

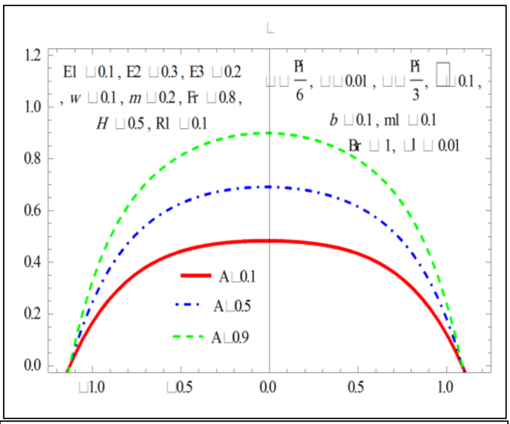

Fig. (8) Temperature profile for variation of A

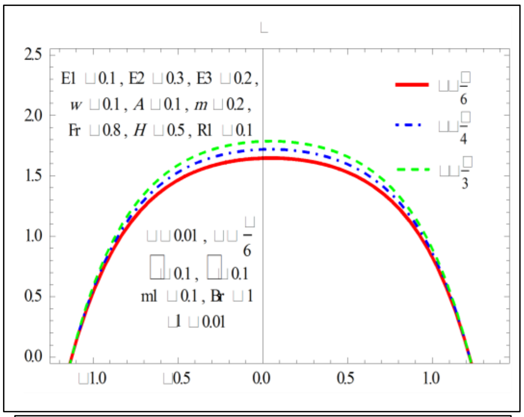

Fig.(9) Temperature Profile Via α

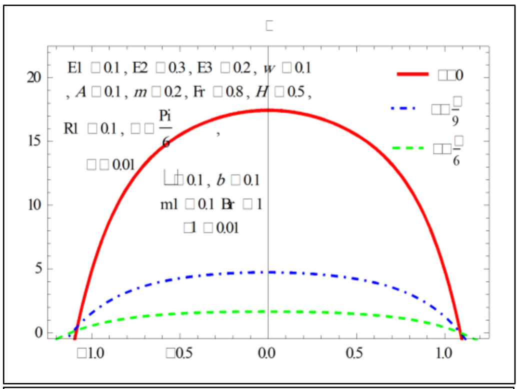

Fig.(10) Temperature Profile Via ϕ

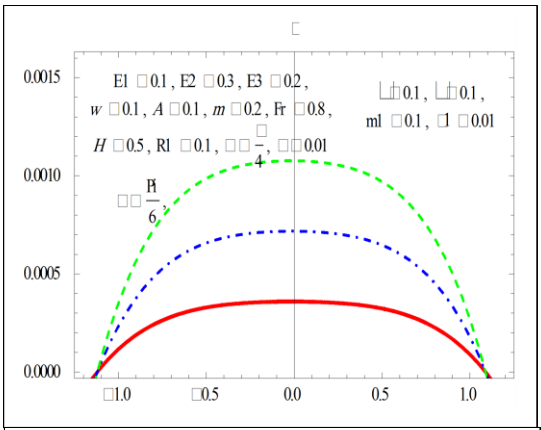

Fig.(11) Temperature Profile Via variation of Br

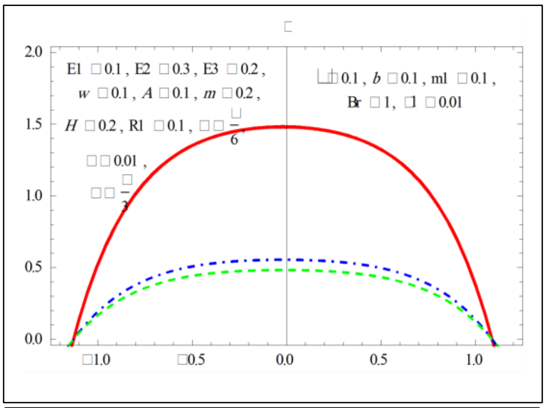

Fig.(12) Temperature Profile Via variation of Fr

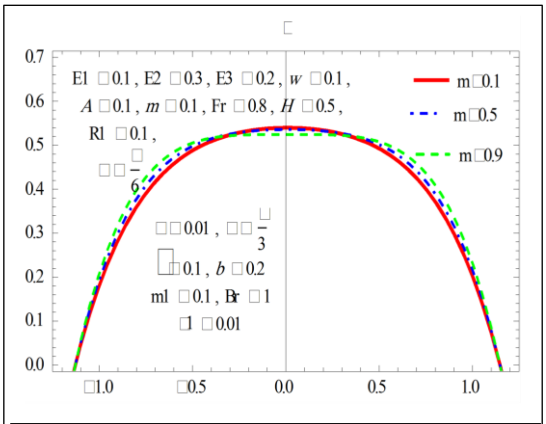

Fig.(18) Temperature profile for m

4.3. Heat Transfer Rate

This subsection considered the development of heat transfer rate $Z(x)$ upon intricate parameters. The magnitude of non-dimensional heat transfer is given at the low wall by applying the inequality $Z(x) = \frac{\partial h_1}{\partial x}\,\theta_y|_{y=h_1}$ for fixed values$(y = 0.2, t = 0.1)$. Figs.(14- 20) shows that the peristaltic waves along the walls produce oscillatory behavior of $Z(x)$. Heat transfer rate (x) . From Fig.(14) we illustrate that the rate of heat transfer has increasing function as the material fluid parameter A becomes larger. Enhancement in heat transfer rate $Z(x)$ is noticed upon increasing both the Brinkman number Br and Hartman parameter via Figs.(15)&(16). According to Figs.(17) & Fig.(18) we observed that the channel inclination α, and Froude number have mixed behavior on $Z(x)$. Fig.(19) study the influence of upper wall amplitude b on rate of heat transfer. It shows that $Z(x)$ increases for ascending values of b. The impact of Hall parameter m on the rate of heat transfer is depicted through the Fig.(20) . Reduction in $Z(x)$ is obtained through the channel with growing up of Hall parameter m.

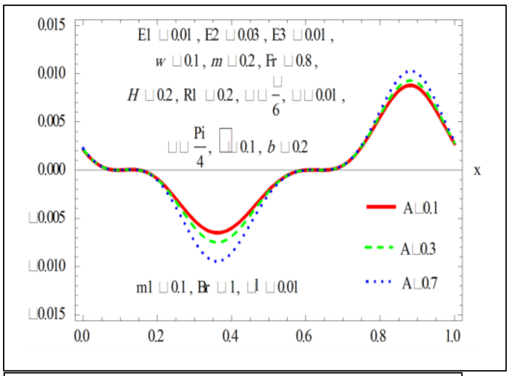

Fig.(14) $Z(x)$ for variation of A

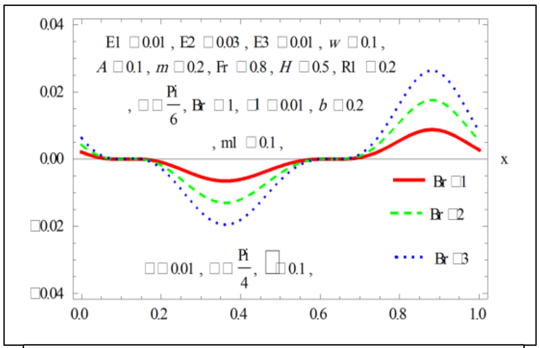

Fig.(15) $Z(x)$ for variation of Br

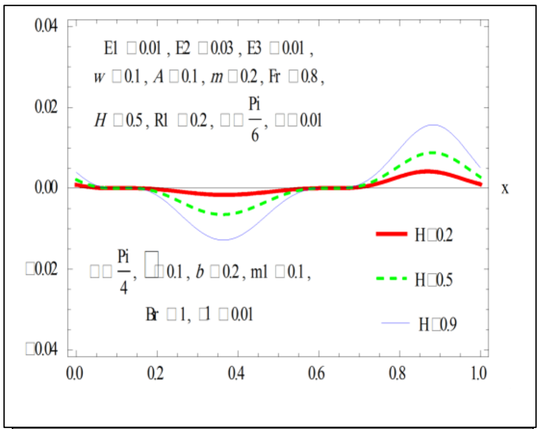

Fig.(16) $Z(x)$ for variation of H

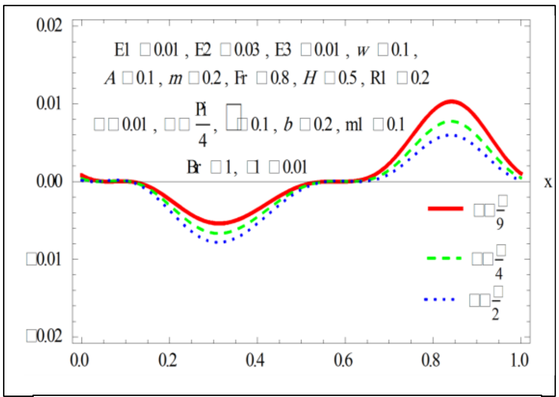

Fig.(17) $Z(x)$ for variation of α

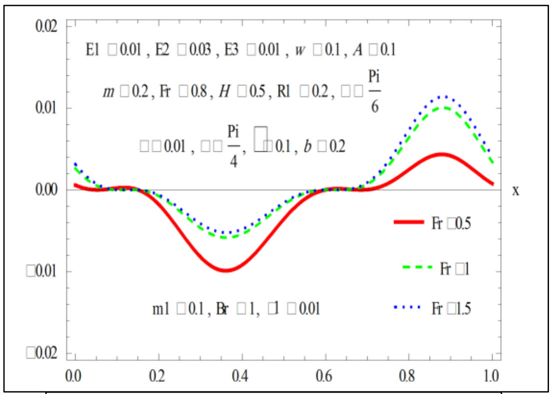

Fig.(18) $Z(x)$ for variation of Fr

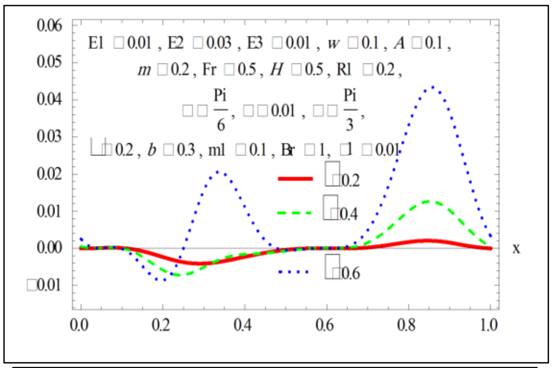

Fig.(19) $Z(x)$ for variation of b

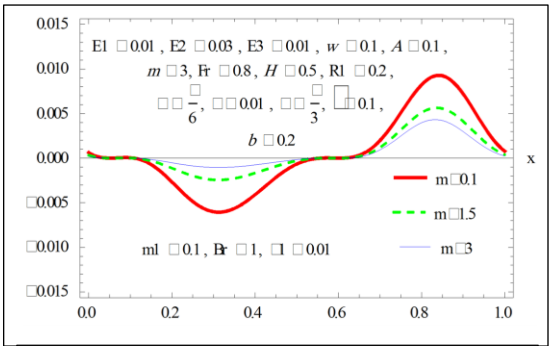

Fig.(20) $Z(x)$ for variation of m

4.4. Trapping Phenomena

In this part, the impact of various effective parameters on stream lines for fixed time $(t = 0.1)$ are furnished in Figs. (21- 28). The interesting phenomenon in peristaltic motion is trapping which refers to the formation of a bolus of fluid that circulates internally and moves with the peristaltic wave at the celerity of waves. The sketches declare that bolus appears near both lower and upper walls in all conditions. It can be visualize from Fig.(21) that when the parameters of wall: rigidity E_1 and tension E_2 increase the size of the bolus increases whilst the number of the trapped bolus remains same. However for ascending values of wall mass parameter E_3 no changes observed on both the size and number of bolus. The impact of material fluid parameter W on the stream lines pattern gained via Fig. (22). The size of trapped bolus extremely decreases whilst the number of bolus increases nears the upper wall and decreases toward the lower wall for larger values of W. It can be scrutinize from Fig.(23) that due to influence of Hall parameter m the size of bolus enhances . The impact of Hartman number H is studied through Fig. (24). It is noticed that larger values of H the bolus becomes smaller. This result is familiar since the Lorentz force opposite the fluid flow and hence reduces the fluid velocity. Fig.(25) is drawn to examine the effect of angle inclination α on streamlines patterns. Enhancement of α enlarge the size of the trapped bolus. Fig.(26) depicts the behavior of the upper wall amplitude b on streamlines. Considerable impact for b on trapped bolus in formulation and size can be noticed. We found that for larger values of b the bolus becomes larger and its form absolutely changes. Fig.(27) revealed that the trapped bolus decreases in size and numbers for higher values of non-uniform channel parameter m_1 . it can be analyzed from Fig.(28) that for higher values of Froude number Fr the size of the trapped bolus decreases and more bolus create near the upper wall opposite situation is seen near the lower wall.

Journal of AL-Qadisiyah for computer science and mathematics Vol.10 No.2 Year 2018
ISSN (Print): 2074 – 0204 ISSN (Online): 2521 – 3504

(a) (b)

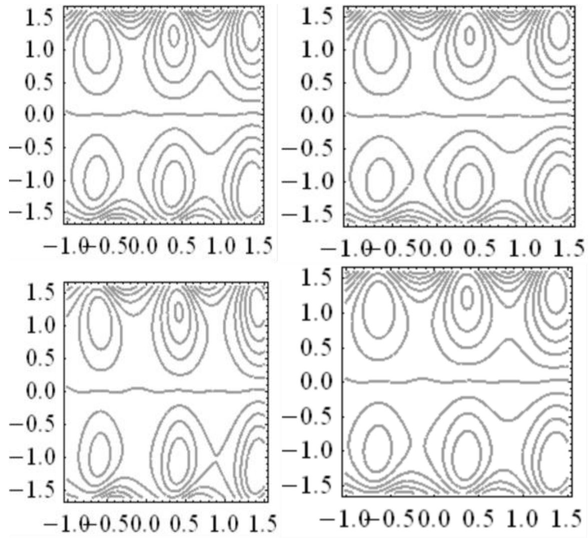

(c) (d)

Fig.(21) Streamlines for $\{w = 0.1, A = 0.1, m = 0.2, \mathrm{Fr} = 0.1, H = 0.5, \mathrm{R1} = 0.2, \alpha = \frac{\pi}{3}, \gamma = 0.01, \phi = \frac{\pi}{6}, \mathrm{a} = 0.1, \mathrm{b} = 0.2, \mathrm{m}_1 = 0.1\}$(a) $(\mathrm{E1} = 0.02, \mathrm{E2} = 0.01, \mathrm{E3} = 0.01)$ (b) $(\mathrm{E1} = 0.04, \mathrm{E2} = 0.01, \mathrm{E3} = 0.01)$ (c) $(\mathrm{E1} = 0.02, \mathrm{E2} = 0.09, \mathrm{E3} = 0.01)$ (d) $(\mathrm{E1} = 0.02, \mathrm{E2} = 0.01, \mathrm{E3} = 0.05)$

(a) (b)

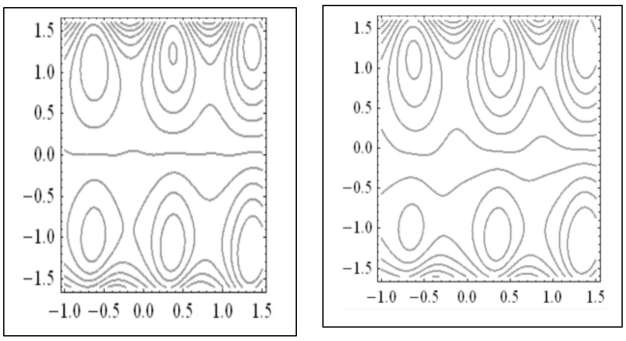

Fig.(22) Streamlines for $\{\mathrm{E1} = 0.02, \mathrm{E2} = 0.01, \mathrm{E3} = 0.01, A = 0.1, m = 0.2, \mathrm{Fr} = 0.1, H = 0.5, \mathrm{R1} = 0.2, \alpha = \frac{\pi}{3}, \gamma = 0.01, \phi = \frac{\pi}{6}, \mathrm{a} = 0.1, \mathrm{b} = 0.2, \mathrm{m}_1 = 0.1\}$ (a)$\mathrm{W} = 0.1$ (b) $\mathrm{W} = 0.5$

(a) (b)

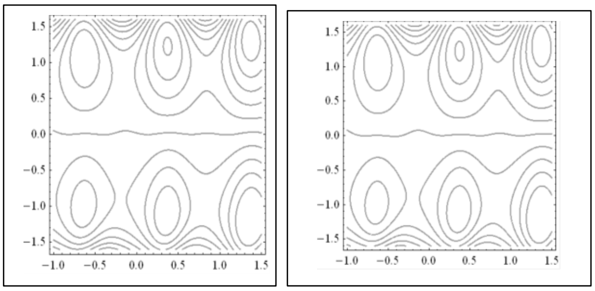

Fig.(23) Streamlines for $\mathrm{E1} = 0.02, \mathrm{E2} = 0.01, \mathrm{E3} = 0.01, W = 0.1, A = 0.1, \mathrm{Fr} = 0.1, H = 0.5, \mathrm{R1} = 0.2, \alpha = \frac{\pi}{3}, \gamma = 0.01, \phi = \frac{\pi}{6}, \mathrm{a} = 0.1, \mathrm{b} = 0.2, \mathrm{m}_1 = 0.1\}$ (a)$\mathrm{m} = 0.2$ (b)$\mathrm{m} = 0.6$

(a) (b)

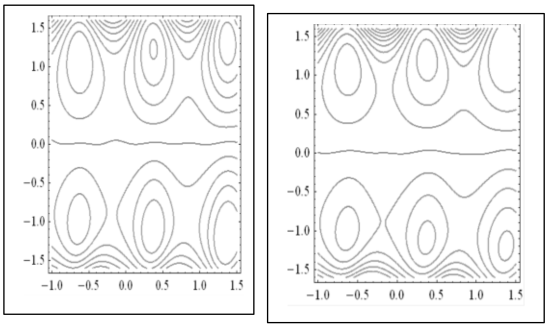

Fig.(24) Streamlines for $\mathrm{E1} = 0.02, \mathrm{E2} = 0.01, \mathrm{E3} = 0.01, W = 0.1, A = 0.1, \mathrm{Fr} = 0.1, m = 0.2, \mathrm{R1} = 0.2, \alpha = \frac{\pi}{3}, \gamma = 0.01, \phi = \frac{\pi}{6}, \mathrm{a} = 0.1, \mathrm{b} = 0.2, \mathrm{m}_1 = 0.1\}$ (a)$\mathrm{H} = 0.2$ (b)$\mathrm{H} = 0.8$

(a) (b)

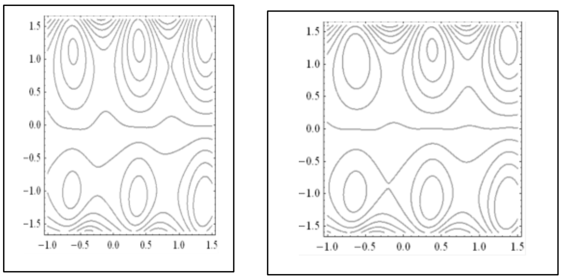

Fig.(25) Streamlines for $\{\mathrm{E1} = 0.02, \mathrm{E2} = 0.01, \mathrm{E3} = 0.01, W = 0.1, A = 0.1, \mathrm{Fr} = 0.1, m = 0.2, \mathrm{R1} = 0.2, H = 0.5, \gamma = 0.01, \phi = \frac{\pi}{6}, \mathrm{a} = 0.1, \mathrm{b} = 0.2, \mathrm{m}_1 = 0.1\}$ (a) $\alpha = \frac{\pi}{6}$ (b)$\alpha = \frac{\pi}{4}$

Journal of AL-Qadisiyah for computer science and mathematics Vol.10 No.2 Year 2018
ISSN (Print): 2074 – 0204 ISSN (Online): 2521 – 3504

(a) (b)

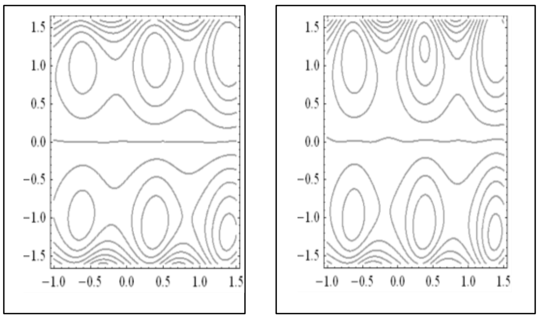

Fig.(26) Streamlines for $\{E1 = 0.02, E2 = 0.01, E3 = 0.01, W = 0.1, A = 0.1, Fr = 0.1, m = 0.2, R1 = 0.2, H = 0.5, \gamma = 0.01, \alpha = \frac{\pi}{3}, \emptyset = \frac{\pi}{6}, a = 0.1, m_1 = 0.1\}$ (a) $b = 0.1$ (b) $b = 0.2$

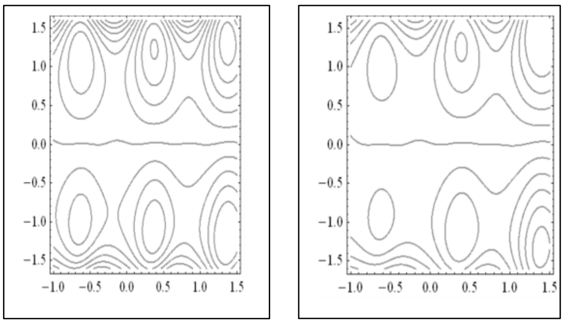

Fig.(27) Streamlines for $\{E1 = 0.02, E2 = 0.01, E3 = 0.01, W = 0.1, A = 0.1, Fr = 0.1, m = 0.2, R1 = 0.2, H = 0.5, \gamma = 0.01, \alpha = \frac{\pi}{3}, \emptyset = \frac{\pi}{6}, a = 0.1, b = 0.2\}$ (a) $m_1 = 0.1$ (b) $m_1 = 0.2$

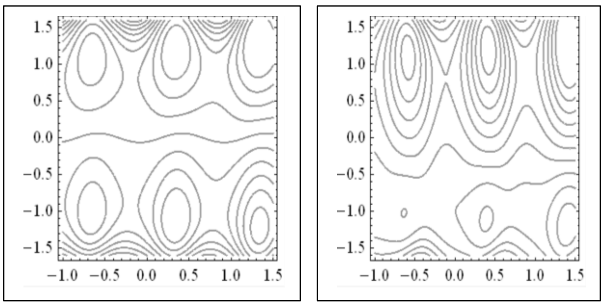

Fig.(28) Streamlines for $\{E1 = 0.02, E2 = 0.01, E3 = 0.01, W = 0.1, A = 0.1, m_1 = 0.1, m = 0.2, R1 = 0.2, H = 0.5, \gamma = 0.01, \alpha = \frac{\pi}{3}, \emptyset = \frac{\pi}{6}, a = 0.1, b = 0.2\}$(a) $Fr = 0.1$ (b)$Fr = 0.2$

5. Concluding Remarks

Peristaltic motion of Powell- Eyring fluid flowing during an inclined tapered symmetric geometry is analyzed. Hall and Ohm's heating effects are taken into account as well as heat transfer phenomenon is discussed. Analytical solutions have been determined using perturbation technique. Major considerations of the analysis have been listed below:

1. Velocity profile shows a parabolic behavior in nature. Furthermore it has an increasing function due to wall parameters E_1 , and E_2, phase difference angle ϕ , Hall parameter m, and non- uniform channel parameter m_1. Whilst a decreasing behavior is recognized via wall parameterE_3, Hartman parameter$H$.
2. The impacts of Powell- Eyring fluid parameters A and W on the velocity field and temperature profile are qualitatively opposite.
3. The temperature profile exhibits an increasing function when Brinkman Br number, and inclination of the channel α increase whereas it decreases with Froude number Fr and phase difference angle ϕ.
4. Hartman number H diminishes the temperature distribution field while mixed results in temperature profile are seen upon Hall parameter m .
5. Heat transfer rate obey an oscillatory behavior for all embedded parameters.
6. Magnitude of heat transfer coefficient gives a mixed function for Froude number Fr , inclination of the channel α.
7. The trapped bolus size occurring in tapered a symmetric channel increasing with Hall parameter m while its size and numbers decrease with Hartman number H.
8. Formulation of fluid bolus is strongly dependent on the non- uniform channel parameter m_1.

References

[1] Akbar, N.S., " Blood flow Suspension in Tapered Stenosed Arteries for Walter's B fluid Model", J. Computer Method and Programs in Biomedicine,132, 45-55,(2016).

[2] Ramesh, K., Devakar, M.," Effect of heat Transfer on the Peristaltic Transport of a MHD Second Grade fluid Through a Porous Medium in an Inclined a Symmetric Channel", Chinese Journal of Physics,55(3),825-844,(2017).

[3] Hayat, T., Aslam,N., Rafiq, M., Alsaadi, F.,"Hall and Joule Heating Effects on Peristaltic Flow of Powell- Eyring Liquid in an Inclined Symmetric Channel" J. Result in Physics,7,518-528,(2017).

[4] Hina,S., Mustafa, M., Hayat, T., Alsaedi, A.,"Peristaltic flow of Powell- Eyring fluid in Curved Channel with Heat Transfer: A useful Application in Biomedicine",J. Computer Method and Programs in Biomedicine,135,89-100,(2016).

[5] Hayat, T.,Bibi, Sh., Alsaadi, F., Rafiq, M.," Peristaltic Transport of Prandtl- Eyring Liquid in a Convectively Heated Curved Channel" J. Plos|one, (2016).

[6] Powell, R.E., Eyring, H., "Mechanisms for the relaxation theory of viscosity," Nature, 154, 427-428, (1944).

[7] Eytan, O., Jaffa, A., Elad, D., "Peristaltic Flow in A Tapered Channel: Application to Embryo Transport Within the Uterine Cavity", J. Medical Engineering and Physics, 23, 473-482, (2001).

[8] Hayat, T., Shafique, M., Tanveer, A., Alsaedi, A., " Magnetohyrodynamic Effects on Peristaltic flow of Hyperbolic Tangent Nanofluid with Slip Condition and Joule heating in an Inclined Channel", International Journal of Heat and Mass Transfer, 102, 54-63, (2016).

[9] Yasmin, H., Hayat, T., Alotaibi, N., Gao, H., " Convective Heat and Mass Transfer Analysis on Peristaltic flow of Williamson fluid with Hall Effects and Joule Heating", International Journal of Biomathematics, 7(5), 1450058(1-7),(2014).

[10] Veerakrishna, M., Swarnalathamma, B., Convective Heat and Mass Transfer on MHD Peristaltic flow of Williamson Fluid with the Effect of Inclined Magnetic Field, International Conference on. Condensed Matter and Applied Physics, 020461-1-020461-8, (2015).

[11] Akbar. N.Sh.," Simulation of Heating Scheme and Chemical Reactions on the Peristaltic Flow of an Eyring- Powell Fluid" J. Int. Numerical Method for Heat and Fluid Flow, 22(6), 764- 776,(2012).

[12] Abbasi, F., Hayat, T., Ahmad, B., "Hydromagnetic Peristaltic Transport of Variable Viscosity Fluid with Heat Transfer and Porous Medium", J. Applied Mathematics and Information Sciences, 10(6),2173-2181,(2016).

[13] Hina, S., "MHD Peristaltic Transport of Eyring- Powell Fluid with Heat/Mass Transfer, Wall Properties and Slip Conditions" Journal of Magnetism and Magnetic Materials,404, 148-158,(2016).

[14] Shapiro, A., Jaffrin, M., & Weinberg, S.," Peristaltic pumping with long wavelength at low Renolds number, ". J. Fluid .Mechanics;37, .799- 825(1969).

[15] Latham, TW.," Fluid Motion in a Peristaltic Pump", Cambridge MA. MIT; (1966).

[16] Hayat, T., Iqbal, R., Tanveer, A., & Alsaedi, A., "Variable Viscosity Effect on MHD Peristaltic Flow of Pseudoplastic Fluid in Tapered A Symmetric Channel", J.Mechanics,(2016).

[17] Kumar, R.," Hydromagnetic Peristaltic Transportation with Porous Medium Through A Symmetric Vertical Tapered Channel and Joule Heating", Application and Applied Mathematics, 11(2), 735- 747, (2016).

[18] Akbar, N.," Non-Newtonian Model Study for Blood Flow Through A Tapered Artery with A Stenosis", Journal of Alexandria Engineering,55, 321- 329,(2016).

[19] Ghosh, S.," MHD Rotating Flow and Heat Transfer Through A Channel with Hall Effect" ,Journal of Magnetism and Magnetic Materials, 404, 221- 229, (2016).

[20] Abass,Z., Naveed, M., Sajid,M., " Nonlinear Radiative Heat Transfer and Hall Effects on A Viscous Fluid in A Semi-Porous Curved Channel" AIP Advances Journal,5,(2015).

تحليل انتقال الحرارة للانتقال الموجي لمائع باول- ايرنك خلال قناة متناظرة مائلة ومدببة مع تأثيرات هول وأوم الحرارية

حياة عادل علي احمد مولود عبدالهادي

جامعة بغداد، كلية العلوم، قسم الرياضيات

المستخلص :

في هذا البحث، ناقشنا مبدأ انتقال الحرارة في الجريان الموجي لمائع باول- ايرنك ضمن قناة مدبب متماثل ومائل. اخذا بنظر الاعتبار تاثير هول، وشرطي الانزلاق للسرعة والحرارة وكذلك تاثير اوم. معادلات الحاكمة لموازنة الكتلة، الحركة والطاقة تم صياغتها ومن ثم تبسيطها اعتمادا على تقريب كبر طول الموجة وصغر عدد رينولد. اخيرا النتائج الصورية اعطيت لتحليل سلوك المتغيرات الوسطية المستجدة في المسالة وقد لوحظ ان تاثير متغير هول وعدد هارتمن يمتلكان خصائص متعارضة على محور السرعة.